

The estimation of functional uncertainty using polynomial chaos and adjoint equations

A. K. Alekseev¹, I. M. Navon^{2,*},[†] and M. E. Zelentsov¹

¹*Moscow Institute of Physics and Technology, Moscow 141700, Russia*

²*Department of Scientific Computing, Florida State University, Tallahassee, FL 32306-4120, U.S.A.*

SUMMARY

The combined use of nonintrusive polynomial chaos (PC) and adjoint equations (yielding the gradient) is addressed aimed at the estimation of uncertainty of a valuable functional subject to large errors in the input data. Random variables providing maximum impact on the result (leading values) may be found using the gradient information that allows reduction of the problem dimension. The gradient may be also used for the calculation of PC coefficients, thus enabling further acceleration of the computations. Copyright © 2010 John Wiley & Sons, Ltd.

Received 18 September 2009; Revised 31 March 2010; Accepted 5 April 2010

KEY WORDS: polynomial chaos; adjoint equations; uncertainty quantification; Hermite polynomials; heat equation; Monte Carlo

1. INTRODUCTION

The estimation of uncertainty of a valuable functional using adjoint equations is considered in several papers, see, for example [1, 2]. The corresponding computational burden does not depend on the number of parameters containing the error, thus providing high computational efficiency. However, formally this approach can be applied only for small errors. The Monte–Carlo method is commonly used for large errors and nonlinear equations, however it requires high computational resources.

The polynomial chaos (PC) expansion [3–25] is often used as an alternative option allowing taking into account the nonlinear effects of large errors. It implies the development of new codes (intrusive approach) or estimation of coefficients from a set of calculations (nonintrusive approach). A number of useful reviews of PC as well as generalized PC(gPC) have been published recently, such as Najm [16], Augustin *et al.* [17], Marzouk and Najm [15] and Xiu [25] to mention but a few.

Intrusive methods are more flexible and, in general, more precise [4, 9, 12–18]. However, the intrusive approach implies the development of new spectral codes that require significant efforts.

Nonintrusive methods of different nature [6–8, 10, 19, 20] are based on running the existing codes that significantly reduce the computational load and provide an opportunity to use the existing well-tested methods.

The general difficulty for all PC-based methods is the ‘curse of dimensionality’. The number of coefficients rapidly increases when the dimension of problem (number of parameters containing random error) and the order of polynomials increase. Significant progress is achieved in reducing the

*Correspondence to: I. M. Navon, Department of Scientific Computing, Florida State University, Tallahassee, FL 32306-4120, U.S.A.

[†]E-mail: inavon@fsu.edu

random space dimension using truncation of Karhunen–Loeve expansion [15, 22, 23]. This approach implies the availability of accurately evaluated covariance matrix, an approach we intend to test in the forthcoming research efforts. Herein, we consider the simpler case of a noncorrelated error.

Significant amount of practical tasks may be specified by certain valuable functionals (maximum temperature, heat flux, drag force, etc.). This functional depends on boundary, initial conditions, coefficients and other problem parameters (input data, see for example [26]) which contain errors and engender the functional uncertainty that is of current interest.

This paper is addressing the issue of estimation of valuable functional uncertainty using a combination of PC and adjoint equations that should partially mitigate the limitations of both the approaches. At the first stage the variables, providing major input in the error of functional, are determined using the gradient obtained via the adjoint equations [11]. This allows us to reduce the dimension of random variables space. In the second stage, the coefficients of expansion over Hermite polynomials are determined using a least-squares nonintrusive variant of PC [6]. The gradient may be also used at this stage to reduce calculations according to [10]. In the final stage, the moments and probability density function are obtained using both the PC expansion (for ‘large’ errors) and the adjoint-based gradient (for ‘small’ errors).

The results of numerical tests are presented for both the linear and nonlinear thermal conduction equations and include moments and the probability density functions.

2. THE ESTIMATION OF UNCERTAINTY OF FUNCTIONAL

Let us consider the estimation of the uncertainty of a functional ε as a function of the input data f_i error. Input data parameters, containing errors, are expressed as $f_i = \langle f_i \rangle + \xi_i \sigma_i$, where ξ_i are the normally distributed random variables with unit variance, σ_i is the standard deviation of f_i . The number of random variables is denoted here as the problem dimension N .

The linear estimate of the valuable functional ε uncertainty may be presented as $\delta\varepsilon = \sum_{i=1}^N \nabla_i \varepsilon \sigma_i \xi_i$ [1, 2], where the gradient $\nabla_i \varepsilon$ is determined using an adjoint problem. This approach directly provides an estimation of the variance. The probability density function may be estimated using the gradient as the meta-model and the Monte–Carlo (MC) method. We use this approach in the numerical tests and denote it as the adjoint Monte–Carlo (AMC).

N_m random values ξ_i , which satisfy the condition $|\nabla_i \varepsilon \sigma_i| > \sigma_*$ (where σ_* is a certain critical magnitude of the error, there is no summation over repeating indexes), are considered as the leading variables (‘large’ errors providing the main input to the total error of the functional).

For the nonlinear estimation of ‘large’ errors’ impact, the function of random variables (functional) is expanded over Hermite polynomials as $\varepsilon = \sum_{i=0}^M b_i H_i(\xi)$. The Hermite polynomials are linked with the normal distribution $\rho(\xi) = (2\pi)^{-N/2} e^{-\xi^2/2}$, $\xi^2/2 = (\xi_1^2 + \dots + \xi_N^2)/2$, ($\xi \in R^N$). They constitute an orthogonal basis in the Gauss measure $\mu(d\xi) = \rho(\xi)d\xi$. Multidimensional Hermite polynomials of the order p may be expressed as

$$H_{i_1, \dots, i_n}^p(\xi_1, \dots, \xi_n) = e^{\xi^* \xi / 2} (-1)^p \frac{\partial^p}{(\partial \xi_1)^{i_1} \dots (\partial \xi_n)^{i_n}} e^{-\xi^* \xi / 2}. \tag{1}$$

In this paper, we use polynomials of the third and fourth orders having the following expressions:

$$\begin{aligned} H^0 &= 1, \\ H^1(\xi_i) &= H_i^1(\xi) = \xi_i, \\ H^2(\xi_{i_1}, \xi_{i_2}) &= H_{i_1 i_2}^2(\xi) = \xi_{i_1} \xi_{i_2} - \delta_{i_1 i_2}, \\ H^3(\xi_{i_1}, \xi_{i_2}, \xi_{i_3}) &= H_{i_1 i_2 i_3}^3(\xi) = \xi_{i_1} \xi_{i_2} \xi_{i_3} - \xi_{i_1} \delta_{i_2 i_3} - \xi_{i_2} \delta_{i_1 i_3} - \xi_{i_3} \delta_{i_1 i_2}. \end{aligned} \tag{2}$$

$$\begin{aligned}
 H_{i_1 i_2 i_3 i_4}^4(\xi) &= \xi_{i_4}(\xi_{i_1} \xi_{i_2} \xi_{i_3} - \xi_{i_1} \delta_{i_2 i_3} - \xi_{i_2} \delta_{i_1 i_3} - \xi_{i_3} \delta_{i_1 i_2}) - \delta_{i_1 i_4} \xi_{i_2} \xi_{i_3} - \delta_{i_2 i_4} \xi_{i_1} \xi_{i_3} \\
 &\quad - \xi_{i_1} \xi_{i_2} \delta_{i_3 i_4} + \delta_{i_1 i_4} \delta_{i_2 i_3} + \delta_{i_2 i_4} \delta_{i_1 i_3} + \delta_{i_3, i_4} \delta_{i_1 i_2}.
 \end{aligned}$$

Fourth-order polynomials were used only for code checking. All the results and expressions used below are presented using only third-order polynomials.

The expansion of the valuable functional is presented in a convenient form in accordance with [10, 12].

$$\varepsilon = b_0 + \sum_{i_1=1}^N b_{i_1} H_{i_1}^1(\xi_{i_1}) + \sum_{i_1=1}^N \sum_{i_2=1}^{i_1} b_{i_1 i_2} H_{i_1 i_2}^2(\xi_{i_1}, \xi_{i_2}) + \sum_{i_1=1}^N \sum_{i_2=1}^{i_1} \sum_{i_3=1}^{i_2} b_{i_1 i_2 i_3} H_{i_1 i_2 i_3}^3(\xi_{i_1}, \xi_{i_2}, \xi_{i_3}). \quad (3)$$

The Cameron–Martin theorem [5] provides for the calculation of the mean value and the variance by the following expressions:

$$E[\varepsilon(\xi)] = b_0, \quad \sigma_\varepsilon^2 = \sum_{i=1}^M b_i^2. \quad (4)$$

In this paper, the random variable space is divided into two subspaces: $\xi_i \in R^{N_m}$ ('large' errors) and $\xi_i \in R^{N-N_m}$ ('small' errors). Correspondingly, the expansion (3) is truncated and assumes the following form:

$$\begin{aligned}
 \varepsilon &= b_0 + \sum_{i_1=1}^{N_m} b_{i_1} H_{i_1}^1(\xi_{i_1}) + \sum_{i_1=1}^{N_m} \sum_{i_2=1}^{i_1} b_{i_1 i_2} H_{i_1 i_2}^2(\xi_{i_1}, \xi_{i_2}) \\
 &\quad + \sum_{i_1=1}^{N_m} \sum_{i_2=1}^{i_1} \sum_{i_3=1}^{i_2} b_{i_1 i_2 i_3} H_{i_1 i_2 i_3}^3(\xi_{i_1}, \xi_{i_2}, \xi_{i_3}) + \sum_{i_1=N_m+1}^N b_{i_1} H_{i_1}^1(\xi_{i_1}). \quad (5)
 \end{aligned}$$

The first three terms account for the 'large' errors, whereas the last term $\sum_{i_1=N_m+1}^N b_{i_1} H_{i_1}^1(\xi_{i_1}) = \sum_{i_1=N_m+1}^N b_{i_1} \xi_{i_1}$ presents the 'small' errors and may be stated as $\sum_{i=N_m+1}^N \nabla_i \varepsilon \sigma_i \xi_i$, that, if necessary, provides the fast calculations using the adjoint-based gradient.

Thus, we determine the most significant part of the error, i.e. the estimate of its nonlinear part using PC, whereas the remaining part of the error is being estimated using a linear approximation by the gradient. In this approach we neglect some part of the series (3) of order greater unit, which accounts for a nonlinear input of 'small' errors, and terms, responsible for the interaction between the 'small' and 'large' errors. This assumption is valid away from the vicinity of singular points (extrema, saddles). We may verify the validity of the leading error selection by carrying out a comparison of the valuable functional $\varepsilon^{(j)} = \varepsilon(\xi_i^{(j)})$ calculated for total random space $\xi_i^{(j)} \in R^N$ and for reduced space $\tilde{\varepsilon}^{(j)} = \varepsilon(\tilde{\xi}_i^{(j)})$, $\tilde{\xi}_i^{(j)} \in R^N$, where $\tilde{\xi}_i^{(j)} = \xi_i^{(j)}$ for $i = 1, N_m$, and $\tilde{\xi}_i^{(j)} = 0$ for $i = N_m + 1, N$.

3. NONINTRUSIVE POLYNOMIAL CHAOS

In general, the calculation of the Hermite expansion entails the development of new codes for spectral mode resolution that requires a very laborious task. In this connection, different variants of the nonintrusive PC [6, 7, 10, 19, 21] are of high current interest. Nonintrusive PC implies the estimation of coefficients using a set of calculations conducted by the standard methods (finite-differences or finite elements) using the existing deterministic codes. We use the stochastic response surface approach [6] in this paper and denote it as PC. We utilize the information on several sets of random vectors $\xi_{i,j} = \xi_i^{(j)} = \xi^{(j)}(x_i)$, where i denotes the number of the vector component ($1 - N$),

j is the number of random vectors in the ensemble $(1 - M)$. The functional $\varepsilon^{(j)}$ is calculated by a run of the main code (heat transfer in this paper).

We may present the ensemble of calculations as

$$\begin{aligned}
 \varepsilon^{(0)} &= b_0 + \sum_{i_1=1}^N b_{i_1} H^1(\xi_{i_1}^{(1)}) + \sum_{i_1=1}^N \sum_{i_2=1}^{i_1} b_{i_1 i_2} H^2(\xi_{i_1}^{(1)}, \xi_{i_2}^{(1)}) \\
 &\quad + \sum_{i_1=1}^N \sum_{i_2=1}^{i_1} \sum_{i_3=1}^{i_2} b_{i_1 i_2 i_3} H^3(\xi_{i_1}^{(1)}, \xi_{i_2}^{(1)}, \xi_{i_3}^{(1)}), \\
 \varepsilon^{(1)} &= b_0 + \sum_{i_1=1}^N b_{i_1} H^1(\xi_{i_1}^{(2)}) + \sum_{i_1=1}^N \sum_{i_2=1}^{i_1} b_{i_1 i_2} H^2(\xi_{i_1}^{(2)}, \xi_{i_2}^{(2)}) \\
 &\quad + \sum_{i_1=1}^N \sum_{i_2=1}^{i_1} \sum_{i_3=1}^{i_2} b_{i_1 i_2 i_3} H^3(\xi_{i_1}^{(2)}, \xi_{i_2}^{(2)}, \xi_{i_3}^{(2)}) \\
 &\quad \vdots \\
 \varepsilon^{(M)} &= b_0 + \sum_{i_1=1}^N b_{i_1} H^1(\xi_{i_1}^{(M)}) + \sum_{i_1=1}^N \sum_{i_2=1}^{i_1} b_{i_1 i_2} H^2(\xi_{i_1}^{(M)}, \xi_{i_2}^{(M)}) \\
 &\quad + \sum_{i_1=1}^N \sum_{i_2=1}^{i_1} \sum_{i_3=1}^{i_2} b_{i_1 i_2 i_3} H^3(\xi_{i_1}^{(M)}, \xi_{i_2}^{(M)}, \xi_{i_3}^{(M)}).
 \end{aligned} \tag{6}$$

Or (by reordering b_j), as

$$A_{ij} b_j = \varepsilon^{(i)}, \quad i = 1, \dots, M+1, \quad j = 0, \dots, M. \tag{7}$$

The system of equations may be stated in an expanded form as

$$\begin{pmatrix}
 1 & H^1(\xi_1^{(1)}) & \dots & H^1(\xi_N^{(1)}) & H_1^2(\xi^{(1)}) & \dots & H_{K_2}^2(\xi^{(1)}) & H_1^3(\xi^{(1)}) & \dots & H_{K_3}^3(\xi^{(1)}) \\
 1 & H^1(\xi_1^{(2)}) & \dots & H^1(\xi_N^{(2)}) & H_1^2(\xi^{(2)}) & \dots & H_{K_2}^2(\xi^{(2)}) & H_1^3(\xi^{(2)}) & \dots & H_{K_3}^3(\xi^{(2)}) \\
 1 & \vdots \\
 1 & H^1(\xi_1^{(M)}) & \dots & H^1(\xi_N^{(M)}) & H_1^2(\xi^{(M)}) & \dots & H_{K_2}^2(\xi^{(M)}) & H_1^3(\xi^{(M)}) & \dots & H_{K_3}^3(\xi^{(M)})
 \end{pmatrix}
 \times
 \begin{pmatrix}
 b_0 \\
 b_1 \\
 \vdots \\
 b_M
 \end{pmatrix}
 =
 \begin{pmatrix}
 \varepsilon_0 \\
 \varepsilon_1 \\
 \vdots \\
 \varepsilon_M
 \end{pmatrix}.$$

Herein, $K_2 = (N^2 + N)/2$, $K_3 = (N^3 + 3N^2 + 2N)/6$, $\xi^{(i)}$ is the random vector and $\xi_j^{(i)}$ denotes random vector components.

Using $M = (N + p)! / N! p!$ runs of the main code with the corresponding number of different random vectors being added to the input data, we may determine the coefficients of system (7), solve it and find b_i ($b_{i_1 i_2 i_3}$). The condition number of the A_{ij} matrix may be controlled by the selection of sample points $\xi_j^{(1)}$.

4. NONINTRUSIVE POLYNOMIAL CHAOS OPTION TAKING INTO ACCOUNT THE GRADIENT

The adjoint equations enable us to calculate the gradient (N variables) of the functional by running a code whose computational cost is similar to that of the forward code. This can accelerate the computation of the PC coefficients for large N . We denote this algorithm as APC. The differentiation of ε over random variables results in the expression

$$\begin{aligned} \frac{\partial \varepsilon}{\partial \xi_\beta} = & \sum_{i_1=1}^N b_{i_1} \frac{\partial H^1(\xi_{i_1})}{\partial \xi_\beta} + \sum_{i_1=1}^N \sum_{i_2=1}^{i_1} b_{i_1 i_2} \frac{\partial H^2(\xi_{i_1}, \xi_{i_2})}{\partial \xi_\beta} \\ & + \sum_{i_1=1}^N \sum_{i_2=1}^{i_1} \sum_{i_3=1}^{i_2} b_{i_1 i_2 i_3} \frac{\partial H^3(\xi_{i_1}, \xi_{i_2}, \xi_{i_3})}{\partial \xi_\beta}, \quad \beta = 1 \dots N. \end{aligned} \quad (8)$$

Here, the left part is obtained from the adjoint problem solving, while the right part is formed by the differentiation of the PC expansion. A single run of the forward and adjoint problems yields $(1 + N)$ relations for first data set $\xi^{(1)}$, given below as

$$\begin{pmatrix} 1 & H^1(\xi_1^{(1)}) & \dots & H^1(\xi_N^{(1)}) & H_1^2(\xi^{(1)}) & \dots & H_{k_2}^2(\xi^{(1)}) & H_1^3(\xi^{(1)}) & \dots & H_{k_3}^3(\xi^1) \\ 0 & \partial H^1(\xi_1^{(1)})/\partial \xi_1 & \dots & \partial H^1(\xi_N^{(1)})/\partial \xi_1 & \partial H_1^2(\xi^{(1)})/\partial \xi_1 & \dots & \partial H_{k_2}^2(\xi^{(1)})/\partial \xi_1 & \partial H_1^3(\xi^{(1)})/\partial \xi_1 & \dots & \partial H_{k_3}^3(\xi^1)/\partial \xi_1 \\ 0 & \vdots \\ 0 & \partial H^1(\xi_1^{(1)})/\partial \xi_N & \dots & \partial H^1(\xi_{N,1}^{(1)})/\partial \xi_N & \partial H_1^2(\xi^{(1)})/\partial \xi_N & \dots & \partial H_{k_2}^2(\xi^{(1)})/\partial \xi_N & \partial H_1^3(\xi^{(1)})/\partial \xi_N & \dots & \partial H_{k_3}^3(\xi^1)/\partial \xi_N \end{pmatrix} \times \begin{pmatrix} b_0 \\ b_1 \\ \vdots \\ b_M \end{pmatrix} = \begin{pmatrix} \varepsilon_0 \\ \partial \varepsilon / \xi_1 \\ \vdots \\ \partial \varepsilon / \xi_N \end{pmatrix}. \quad (9)$$

We need $\sim M/N$ cycles of calculations to obtain the closed system

$$A_{ij} b_j = f_i, \quad i = 1, \dots, M+1, \quad j = 0, \dots, M. \quad (10)$$

(In real applications, we usually obtain an overdetermined system.)

This approach provides approximately an N -fold reduction of the computation time when compared with the PC.

The coefficients b_j readily provide us with $\bar{\varepsilon}$ and σ using Equation (4). The probability density function $P(\varepsilon)$ is also easily obtained by generating ξ and calculating ε using the polynomial presentation (5) as a meta-model. This approach is illustrated below for the linear and nonlinear heat transfer equations.

5. TEST PROBLEMS

Let us consider the thermal conduction model

$$\begin{aligned} C \frac{\partial T}{\partial t} - \frac{\partial}{\partial x} \left(\lambda \frac{\partial T}{\partial x} \right) &= 0, \\ T(0, t) &= T_w, \quad T(X, t) = T_R, \\ T_{t=0} &= T_0(x), \end{aligned} \quad (11)$$

where $T(t, x)$ is the temperature, C is the volume heat, λ is the thermal conductivity, and X is the specimen thickness.

The estimated functional

$$\varepsilon = \int_0^T T \delta(x - x_{\text{est}}) \delta(t - t_{\text{est}}) dx dt. \quad (12)$$

Herein, $x_{\text{est}}, t_{\text{est}}$ determine the coordinate for pointwise temperature estimation (in applications, it may be the temperature at an important moment in a sensitive place (payload, etc.)). The choice of functional is task dependent, here we use the simplest one without the loss of generality.

We search for moments and probability density function of the functional caused by a normally distributed error in the thermal conductivity or the initial state.

For gradient calculation we employ the function $\Psi(t, x)$, obtained via solution of the following adjoint problem

$$C \frac{\partial \Psi}{\partial t} + \lambda \frac{\partial^2 \Psi}{\partial x^2} - \delta(t - t_{\text{est}}) \delta(x - x_{\text{est}}) = 0, \quad (13)$$

$$\text{Boundary conditions: } \frac{\partial \Psi}{\partial x} \Big|_{x=X} = 0, \quad \frac{\partial \Psi}{\partial x} \Big|_{x=0} = 0, \quad (14)$$

$$\text{Final condition: } \Psi(t_f, x) = 0. \quad (15)$$

The gradient of the functional related to an initial temperature is $\nabla \varepsilon = \Psi(0, x)$ and regarding the conductivity coefficient is $\int \Psi (\partial^2 T / \partial x^2) dt dx$. This gradient is connected with derivatives of the functional over random variables in T_0 :

$$\frac{\partial \varepsilon(\xi^{(m)})}{\partial \xi_i} = \frac{\partial \varepsilon}{\partial T_{0,i}} \frac{\partial T_0}{\partial \xi_i} = \Psi(0, x_i) \sigma_i, \quad (16)$$

and in λ :

$$\frac{\partial \varepsilon}{\partial \xi_i} = \frac{\partial \varepsilon}{\partial \lambda} \frac{\partial \lambda}{\partial \xi_i} = \int \Psi \frac{\partial^2 T}{\partial x^2} \sigma_i dx dt. \quad (17)$$

In the first test problem we consider four random variables in the thermal conductivity $\lambda = \bar{\lambda} + \sigma_i \xi_i$. Here, ξ_i are the random variables with the normal distribution of unit variance. The variation of functional is presented as

$$\delta \varepsilon = \varepsilon - \langle \varepsilon \rangle = \int_0^T \int_{\Omega} \sum_i \Psi \frac{\partial^2 T}{\partial x^2} \sigma_i \xi_i dx dt. \quad (18)$$

In a second test problem the initial data contain the normally distributed error: $T_0(x_i) + \delta T_0(x_i) = T_0(x_i) + \sigma_i \xi_i$. In this test (in linear case when $\lambda(T) = \lambda_1 = \text{Const}$), $\nabla \varepsilon = \Psi(0, x)$ does not depend on T_0 . So, the gradient information cannot be used in (10) and APC cannot be applied.

In a third test problem the thermal conductivity is a nonlinear function assuming the following form $\lambda(T) = \lambda_0 + \lambda_1 (T/T_s)^3$, (for $T < 0, \lambda(T) = \lambda_0$). The initial data contain the normally distributed error: $T_0(x_i) + \delta T_0(x_i) = T_0(x_i) + \sigma_i \xi_i$.

6. NUMERICAL RESULTS

The heat transfer equation and adjoint equation of tests were solved by conservative finite difference scheme of the second order over the space and time [27].

In numerical tests we used MC, Monte-Carlo using gradient (AMC), nonintrusive polynomial chaos (PC) and polynomial chaos methods using adjoint equations (APC).

Systems (7) and (10) were solved using a singular value decomposition (SVD) [28]. So, the approach considered herein may be classified as belonging to linear regression (stochastic response surface) methods [19]. SVD may be considered as a variant of least-squares problem solvers,

and it may be used for overdetermined system of equations. The time consumed by SVD was negligible when compared with the time required for solving direct (11) or adjoint (13) problems. Oversampling is known [21] to improve the quality of solution for stochastic response surface methods, so it may be used in this approach in a natural way.

Moments and the probability density function were calculated using from 10 000 to 600 000 samples.

6.1. Error in thermal conductivity

Figure 1 presents probability density functions $P(T)$ of the functional obtained using MC, AMC and PC. The thermal conductivity contained four normally distributed random variables with the standard deviation equal to $0.1 \cdot \bar{\lambda}$. PC method was implemented using a third-order polynomial. All tests used 100 000 samples.

The comparison of mean values $\bar{\varepsilon}$ and standard deviations σ is presented in Table I. This table also contains the computation cost (consumed time normalized by the time of single problem run).

The nonintrusive PC exhibits a relatively smaller accuracy when compared with MC and AMC methods and a much smaller computational efficiency when compared with AMC. The moments calculated from PC coefficients by the Cameron–Martin theorem (Table I, A) and the MC simulation using PC as a meta-model (Table I, B) are similar.

6.2. Initial temperature error. Linear case

Let us consider the influence of an initial temperature error on the final temperature at a reference point. The final temperature distribution is presented in Figure 2. The reference point is number $k = 54$, the error being added to all points of the initial temperature distribution ($N = 100$).

Figure 3 presents the PC results in comparison with MC for an input data error with a standard deviation that equals 10. PC3-PC11 denotes the PC and the number of accounted variables.

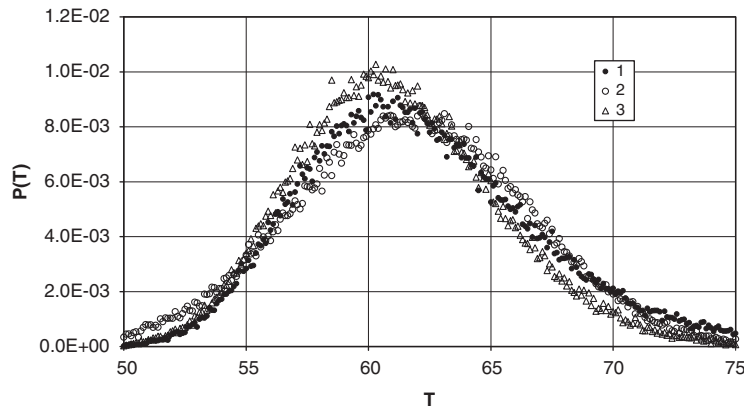


Figure 1. Probability density. 1-MC, 2-AMC, and 3-PC.

Table I. Comparison of mean values, standard deviation and the computational cost for MC, AMC and PC methods, respectively.

	MC	AMC	PC	
			A	B
$\bar{\varepsilon}$	62.285	61.776	61.247	61.269
Standard deviation σ	4.971	4.783	4.174	4.168
Computation cost	100000	2	35	

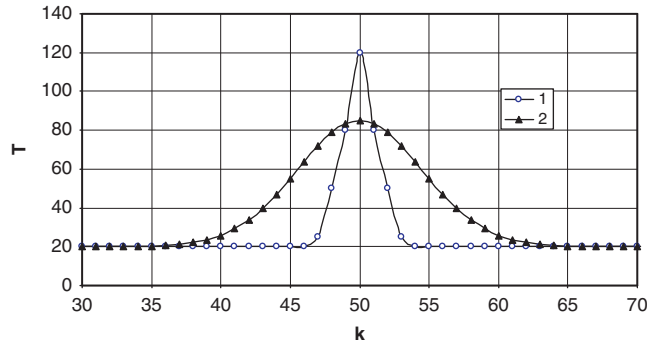


Figure 2. Distribution of temperature over space at the initial time (1) and final time (2) for error-free data.

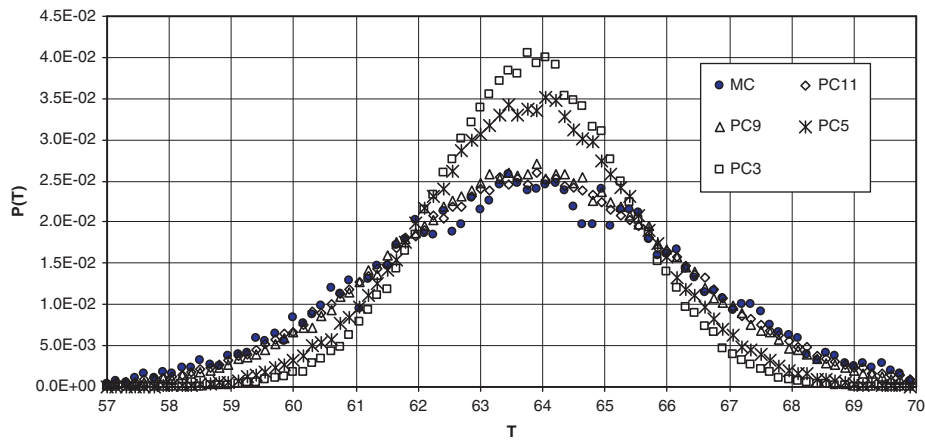


Figure 3. Probability density at reference point (100 000 trials)

Increasing the number of accounted nodes improves the quality of the result. A good agreement between MC and PC is observed when the number of nodes (containing error) is nine or higher.

A good agreement between PC with MC and AMC may be achieved using only three leading vectors if the linear terms (obtained using adjoint problem) are accounted for; see Figure 4 which confirms an equivalence of PC and AMC in the linear case. Herein, PC3+ denotes PC taking into account 3 nodes and adjoint derived linear terms over the remaining ones. For those nodes, where PC coefficients were calculated, a good coincidence of first-order PC coefficients and gradient-based data $b_i \approx \nabla_i \varepsilon \sigma_i$ is observed. Table II presents the mean values and standard deviations for the above mentioned tests.

In general, for the linear case, AMC is significantly superior to other methods in as far as the computation time for similar accuracy requirement is concerned.

6.3. Impact of initial temperature error. Nonlinear case

The above tests demonstrated the validity of considered methods for linear case; however, the potential benefits of PC in the comparison with another approaches may also be detected in the nonlinear case. The test problem considered below is characterized by the cubic dependence of the thermal conductivity coefficient on the temperature; (see Figure 5). This provides a significant nonlinear effect for heat localization (Figure 6) ($T_s = 25$).

Figure 6 presents the temperature distribution at the final moment. A comparison with Figure 2 clearly demonstrates the influence of nonlinearity.

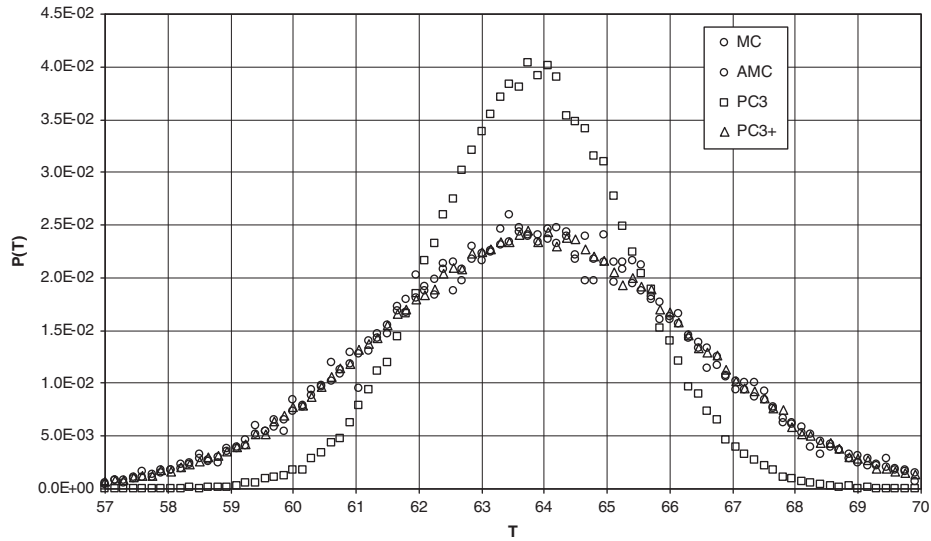


Figure 4. Probability density at reference point (100 000 trials) with account of linear (gradient) terms.

Table II. Comparison of mean values, standard deviations and computational costs of PC, AMC and PC3-PC11 (number of accounted for nodes) methods, respectively.

	MC	AMC	PC3+	PC3	PC5	PC9	PC11
Mean	63.881	63.906	63.888	63.889	63.883	63.887	63.888
Standard deviation	2.491	2.507	2.512	1.517	1.742	2.279	2.382
Computation cost	100000	2	22	20	56	220	364

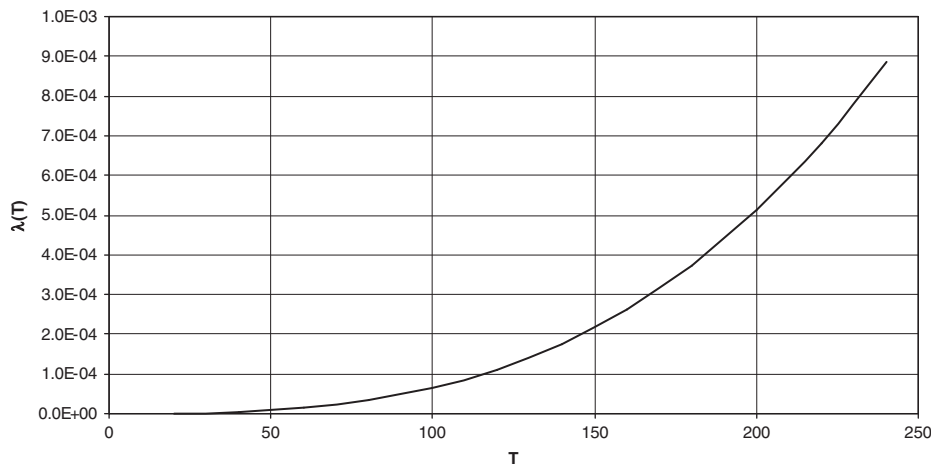


Figure 5. Thermal conductivity as a function of temperature.

Figure 7 presents the gradient of the functional for the nonlinear case providing an opportunity to select leading vectors (in the linear tests the adjoint-based gradient was found to be more reliable).

If only a single point contains the error, the nonlinearity significantly distorts the probability distribution as compared with the Gaussian. Figure 8 presents the probability distribution for the temperature, measured at point $k=54$ when a normally distributed error is applied at $k=48$. The results are obtained by MC, AMC and PC for a standard deviation 50.0 ($\sigma/T_s = 2$). The distribution

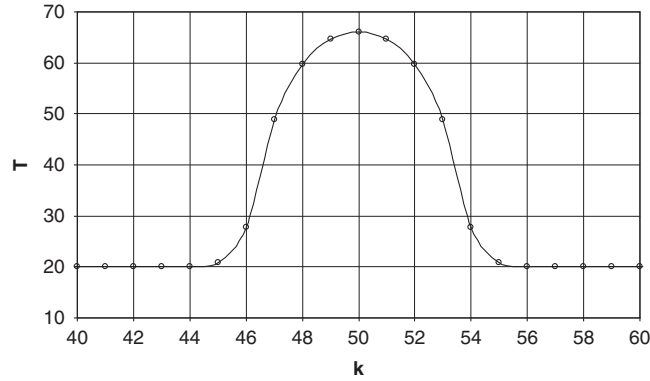


Figure 6. Final temperature distribution for nonlinear problem.

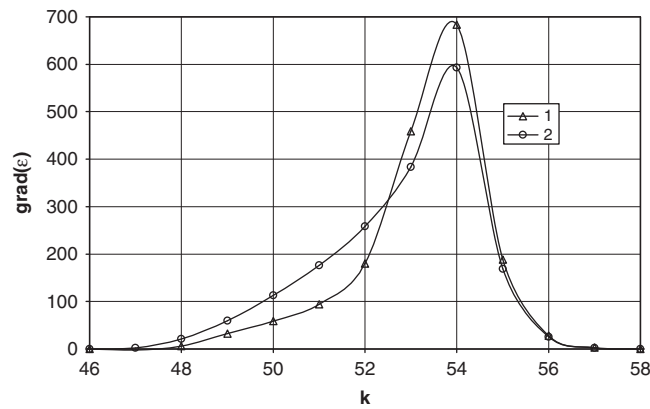


Figure 7. 1—Gradient obtained by direct numerical differentiation, and 2—gradient obtained using adjoint equations.

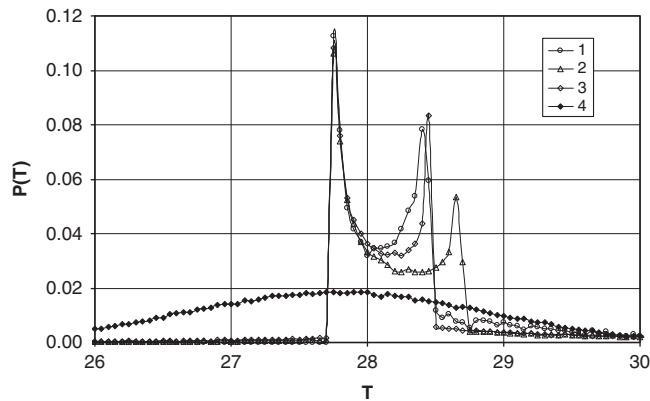


Figure 8. Probability density of functional for single point containing the error. 1-MC, 2,3-PC with different sets of sample points, 4-AMC.

calculated by AMC qualitatively deviates from MC. PC provides a much more acceptable result. Unfortunately, the result significantly varies depending on the selection of interpolation points $\zeta^{(i)}$. Figure 8 provides the results for two different sets of $\zeta^{(i)}$.

If all points of the initial distribution contain the error, the qualitative picture changes significantly and the influence of nonlinearity is smeared. Figures 9–12 present results for the test where every

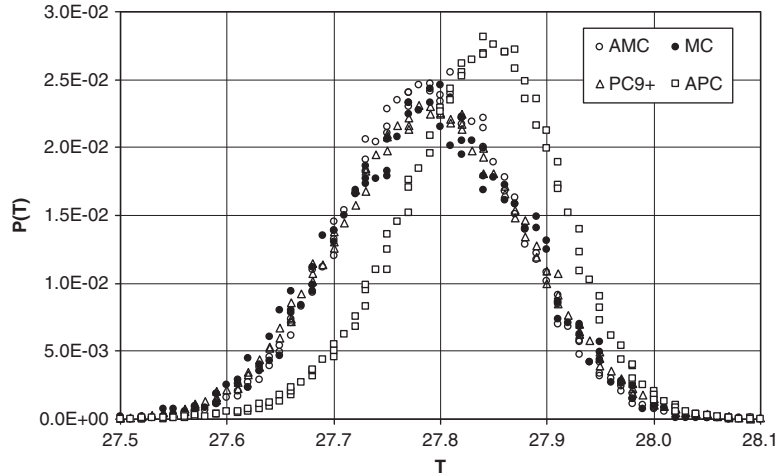


Figure 9. Calculations for initial temperature with the standard deviation 0.1.

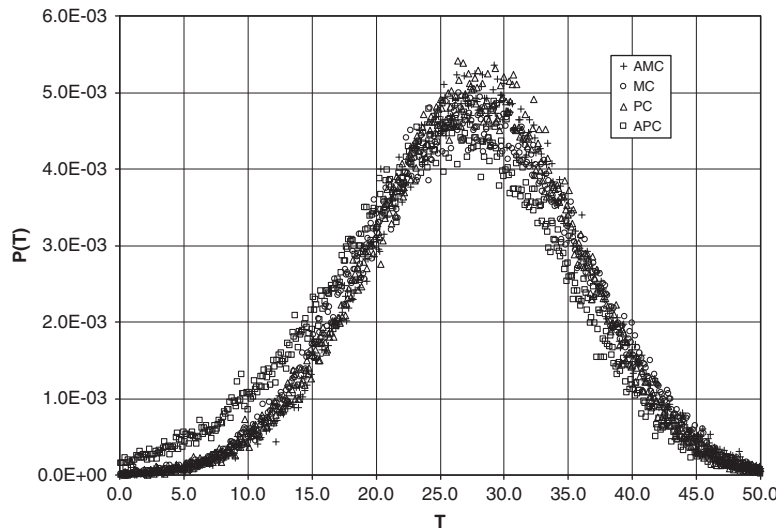


Figure 10. Probability density for initial temperature with a standard deviation 10.0 (9 nodes).

point of the initial temperature contains an error with the same variance. Figure 9 presents results by MC and AMC for an initial temperature error with a standard deviation of 0.1. PC yields good results, while the APC results are slightly worse.

Figure 10 presents calculations by MC, AMC, PC and APC (50 000 trials) for an initial temperature error with a standard deviation of 10.0 ($\sigma/T_s = 0.4$).

Figure 11 presents calculations by MC, AMC, PC and APC (50 000 trials) for an initial temperature error with the standard deviation 50.0 ($\sigma/T_s = 2$). PC and APC provide a slightly more accurate result when compared with AMC; however, there is no total coincidence with MC.

Unfortunately, the choice of an ‘unlucky’ matrix of observations may cause PC to provide much less accurate results, a comparison for five different sets $\zeta_j^{(1)}$ is provided in Figure 12. All matrices were well conditioned, so the source of deviations is the unknown shape of $\varepsilon(\zeta)$.

Oversampling [21] was used to cure the influence of selection of sample points; Figure 13 demonstrates the stability of results with a twofold oversampling, and nevertheless, the computational cost significantly grows, a fact that reduces the advantage of PC.

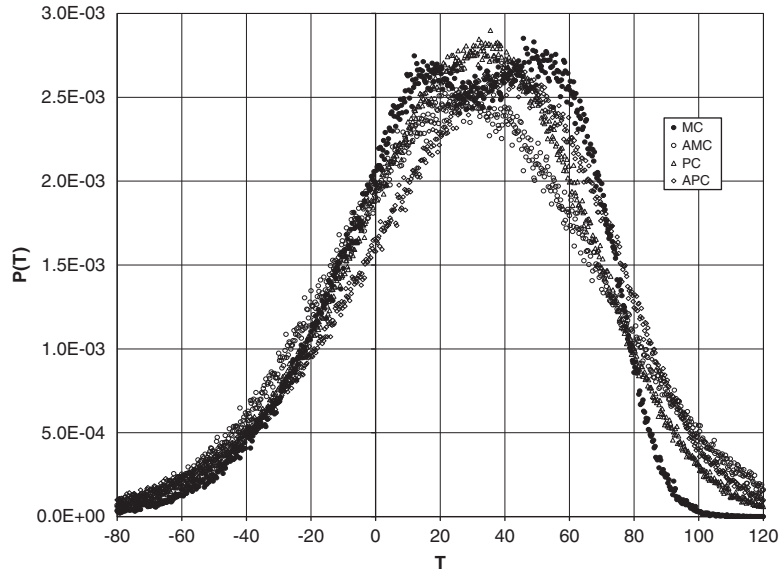


Figure 11. Probability density for the initial temperature with a standard deviation 50.0 (9 nodes).

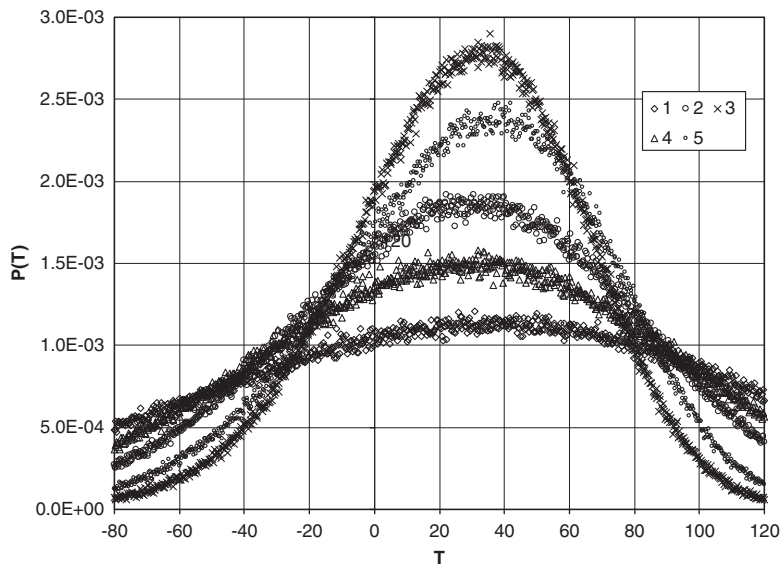


Figure 12. Probability density for five different sets of sample points $\zeta_j^{(1)}$ without oversampling.

7. DISCUSSION

The number of coefficients of polynomials $M = (N + p)!/N!p!$ increases rapidly when the polynomial order p and the number of random variables N increases. For example, 15 random variables and a third order of polynomial require 816 coefficients, so the computational burden approaches the one required by the MC method. Some additional means, considered in this paper, may be used for improving the PC performance. The use of leading variables provides the possibility for a rapid decrease of N . The gradient (obtained via adjoint equations) enables to reduce the computational cost order by an order of magnitude (in this paper from cubic to quadratic dependence on N). Unfortunately, a reliable identification of small error subspace in the global sense

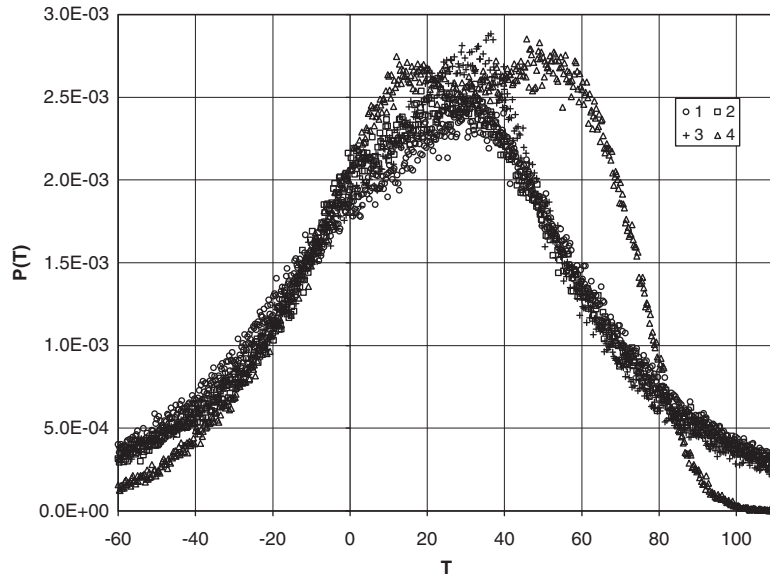


Figure 13. 1, 2, 3—Probability density for different sets of sample points $\xi_j^{(1)}$ with two-fold oversampling, 4—Monte–Carlo.

for genuine nonlinear problem is close to impossible. Some additional trials may be used to check the correctness of the determination of small error subspace in the domain of interest.

The considered variant of nonintrusive PC is based on the interpolation of the set of solutions $\varepsilon^{(j)}$ in multidimensional space of $\xi_i^{(j)}$ via the estimation of polynomial coefficients. The quality of this interpolation depends on the condition number of the matrix $A(i, j)$ (which is verified by the singular values obtained in solving the system of equations by SVD) and on the properties of $\varepsilon(\xi_i)$ that are unknown in the general case. Nodes (sampling points) $\xi_i^{(j)}$ may be occasionally allocated in a region, which purely reflects the geometry of $\varepsilon(\xi_i)$ that may cause a large interpolation error. The oversampling reduces the influence of the selection of sampling points at the cost of an increase in the number of $\varepsilon^{(j)}$ calculations.

8. CONCLUSION

The estimation of variables providing the main input to the total error of the functional using adjoint equations provides an opportunity for obtaining a rapid reduction of the dimension of the random space and, respectively, the number of polynomial coefficients used in the Hermite series. This enables a reduction in the computational burden for nonintrusive Polynomial Chaos applications.

Using gradient information for the estimation of polynomial coefficients (APC) also provides a significant reduction of the computation time.

The adjoint Monte–Carlo is highly efficient from a computational viewpoint and accurate for moderate amplitude of errors. For a large number of random variables, the accuracy of AMC is close (or even superior) to PC results even under large errors.

REFERENCES

1. Ghate D, Giles MB. *Inexpensive Monte Carlo Uncertainty, SAROD-2005*. McGraw-Hill: New York, 2005.
2. Alekseev AK, Navon IM. On estimation of temperature uncertainty using the second order adjoint problem. *International Journal of Computational Fluid Dynamics* 2002; **16**(2):113–117.
3. Wiener N. The homogeneous chaos. *American Journal of Mathematics* 1938; **60**:897–936.
4. Ghanem RG, Spanos PD. *Stochastic Finite Elements: A Spectral Approach*. Dover: New York, 2003.

5. Cameron RH, Martin WT. The orthogonal development of non-linear functionals in series of Fourier–Hermite functionals. *Annals of Mathematics* 1947; **48**:385–392.
6. Hosder S, Walters RW, Perez R. A non-intrusive polynomial chaos method for uncertainty propagation in CFD simulations. *AIAA 2006-891*, 2006; 1–19.
7. Mathelin L, Hussaini MY. A stochastic collocation algorithm for uncertainty analysis. *Technical Report NASA/CR-2003-212153*, NASA Langley Research Center, 2003.
8. Mathelin L, Hussaini M, Zang T. Stochastic approaches to uncertainty quantification in CFD simulations. *Numerical Algorithms* 2005; **38**:209–236.
9. Hou TY, Luo W, Rozovskii B, Zhou H-M. Wiener Chaos expansions and numerical solutions of randomly forced equations of fluid mechanics. *Journal of Computational Physics* 2006; **216**:687–706.
10. Isukapalli SS, Roy A, Georgopoulos PG. Efficient sensitivity/uncertainty analysis using the combined stochastic response surface method and automatic differentiation. *Risk Analysis* 2000; **20**:591–602.
11. Wang Q, Chantrasmith T, Iaccarino G, Moin P. Adaptive uncertainty quantification using adjoint method and generalized polynomial chaos. *59th Annual Meeting of APS Division of Fluid Dynamics*, Tampa Bay, 2006.
12. Xiu D, Karniadakis GE. The Wiener–Askey polynomial chaos for stochastic differential equations. *SIAM Journal on Scientific Computing* 2002; **24**:619–644.
13. Xiu DB, Karniadakis GE. Modeling uncertainty in flow simulations via generalized polynomial chaos. *Journal of Computational Physics* 2003; **187**:137–167.
14. Wan X, Karniadakis GE. An adaptive multi-element generalized polynomial chaos method for stochastic differential equations. *Journal of Computational Physics* 2005; **209**:617–642.
15. Marzouk YM, Najm HN. Dimensionality reduction and polynomial chaos acceleration of Bayesian inference in inverse problems. *Journal of Computational Physics* 2009; **228**:1862–1902.
16. Najm HN. Uncertainty quantification and polynomial chaos techniques in computational fluid dynamics. *Annual Review of Fluid Mechanics* 2009; **41**:35–52.
17. Augustin F, Gilg A, Paffrath M, Rentrop P, Wever U. Polynomial chaos for the approximation of uncertainties: chances and limits. *European Journal of Applied Mathematics* 2008; **19**:149–190.
18. Le Maitre OP, Najm HN, Ghanem RG, Knio OM. Multi-resolution analysis of Wiener-type uncertainty propagation schemes. *Journal of Computational Physics* 2004; **197**:502–531.
19. Eldred MS, Burkardt J. Comparison of non-intrusive polynomial chaos and stochastic collocation methods for uncertainty quantification. *AIAA Paper 2009-0976*, 2009; 1–20.
20. Loeven GJA, Witteveen JAS, Bijlz H. Probabilistic collocation: an efficient non-intrusive approach for arbitrarily distributed parametric uncertainties. *AIAA Paper 2007-317*, 1–14.
21. Debusschere BJ, Najm HN, Pebay P, Knio OM, Ghanem RG, Le Maitre OP. Numerical challenges in the use of polynomial chaos representations for stochastic processes. *SIAM Journal on Scientific Computing* 2004; **26**:698–719.
22. Doostan A, Ghanem RG, Red-Horse J. Stochastic model reduction for chaos representations. *Computer Methods in Applied Mechanics and Engineering* 2007; **196**:3951–3966.
23. Lu Z, Zhang D. A comparative study on uncertainty quantification for flow in randomly heterogeneous media using Monte Carlo simulations and conventional and KL-based moment-equation approaches. *SIAM Journal on Scientific Computing* 2004; **26**(2):558–577.
24. Rupert CP, Miller CT. An analysis of polynomial chaos approximations for modeling single-fluid-phase flow in porous medium systems. *Journal of Computational Physics* 2007; **226**:2175–2205.
25. Xiu D. Fast numerical methods for stochastic computations: a review. *Communications in Computational Physics* 2009; **5**(2–4):242–272.
26. Wright MJ, Bose D, Chen Y-K. Probabilistic modeling of aerothermal and thermal protection material response uncertainties. *AIAA Journal* 2007; **45**(2):399–410.
27. Samarskii AA. *Theory of Difference Schemes*. Marcel Dekker: NY, 2001.
28. Press WH, Flannery BP, Teukolsky SA, Vetterling WT. *Numerical Recipes in Fortran 77: The Art of Scientific Computing*. Cambridge University Press: Cambridge, 1992.